August 27-31, 2023
FLORENCE - ITALY
ICWE 16
16th International Conference on Wind Engineering

Comparison of load characteristics of a high-rise building under synoptic and non-synoptic wind profiles

Zhenjiang Jin [1], Jinxin Cao [1,2], Shuyang Cao [1,2]

[1] *College of Civil Engineering, Tongji University, Shanghai, China*
[2] *State Key Lab of Disaster Reduction in Civil Engineering, Tongji University, Shanghai, China*

SUMMARY:
This paper compares aerodynamic load characteristics of a 1:200 high-rise building model under synoptic and non-synoptic wind profiles through rigid model wind pressure measurements. The wind profiles including both synoptic and non-synoptic ones were reproduced in a multiple-fan actively-controlled wind tunnel. Aerodynamic load characteristics including surface wind pressure distributions, interlayer wind forces and overall wind forces were mainly discussed.

Keywords: non-synoptic wind profiles, high-rise building, load characteristics

1. INTRODUCTION

In recent years, extreme weather disasters such as tornadoes and thunderstorms have occurred frequently, which can cause serious damage to building structures and significant losses to people's lives and properties. Researches on wind loads and responses of high-rise buildings under synoptic wind profiles (Atmospheric boundary layer wind, ABL) has been systematically investigated (Zhang et al, 2014), but knowledge about such characteristics under non-synoptic wind profiles such extreme weather above is quite limited. In this paper, rigid model wind pressure measurements on a high-rise building was carried out for both synoptic and non-synoptic wind profiles in a multiple-fan actively-controlled wind tunnel, and aerodynamic load characteristics under these two types of wind profiles were mainly investigated, in terms of surface wind pressure distributions, interlayer and overall wind forces over the building model.

2. EXPERIMENTAL SETTINGS

In the multiple-fan actively-controlled wind tunnel, we reproduced four types of synoptic wind profiles based on the wind load standards, and 12 tornado wind profiles recommended in (El Damatty & Hamada, 2016; Hamada et al, 2010; Kashefizadeh et al, 2019), considering variations in their turbulence intensities (8-20%) and turbulence integral scales. (See Table.1)

Table 1. Turbulence features of non-synoptic wind profiles.

No	1	2	3	4	5	6	7	8	9	10	11	12
I_u	8%	8%	8%	11%	11%	11%	15%	15%	15%	20%	20%	20%
L_{ux}/m	0.58	0.70	0.85	0.52	0.72	0.78	0.63	0.74	0.91	0.57	0.77	0.89

The geometric scale of the tested model is 1:200, corresponding to a 24m(L) × 24m(B) × 120m(H) prototype building. There are 6 × 15 = 90 pressure taps on each surface of the four side surfaces, and 6 × 6 = 36 on the top. 10 wind directions (from 0° to 45° with a five-degree increment) were measured for each wind profile case. (See FIG.1)

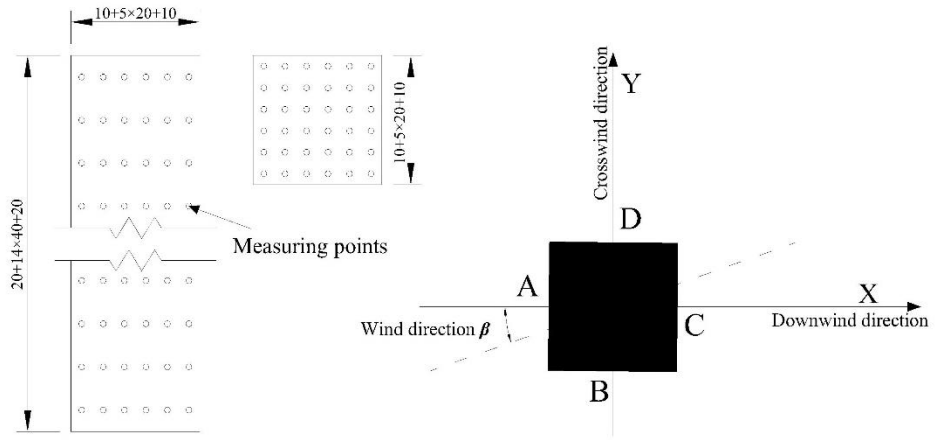

Figure 1. Building model and working condition diagram (unit: mm)

3. RESULT

3.1. Wind pressure coefficient distribution

For wind pressure and force coefficient calculation, the maximum wind speeds within the height of the building model for respective wind profiles were used as the reference wind speeds. The maximum wind speeds for the boundary layer wind profiles are recorded at the top of the building, while they occur in the middle part of the building for the tornado wind profiles (see FIG.2). Since the reference wind speeds were measured at the top of the building for both types of wind profiles in the experiments, a conversion factor η=0.84 was used with the wind speed at the top of the building U_{top} = 8.16 m/s, and the maximum wind speed U_{max}=8.90 m/s.

FIG.2 presents the distribution of mean wind pressure coefficients on the surface of the building model under different wind profiles (a: Terrain category A profile in Chinese code, b: tornado wind profile #2) simulated in the multiple-fan wind tunnel. For the results on the windward side of the building (face A), the location of the most unfavorable wind pressure coefficient under the non-synoptic wind profile is significantly lower than the results under the synoptic wind profile, which is obviously due to the fact that the location of maximum wind speed in the non-synoptic wind profile is lower than that in the synoptic wind profile. The results for the two side surfaces of the building (face B and D) show that the non-synoptic wind profile result has more significant variations in negative pressure at the bottom corner of the building compared to the synoptic, which is originated from large vertical wind shear at the bottom of the non-synoptic wind profile; meanwhile, the magnitude of negative pressure at the middle part close to face C are also larger for the non-synoptic wind profile. For the results on the leeward side of the building (face C), the difference between the two wind profiles is not as obvious as the results on the windward side, and the locations of the most unfavorable negative pressure values are similar for both, which are basically located in the middle of the building surface.

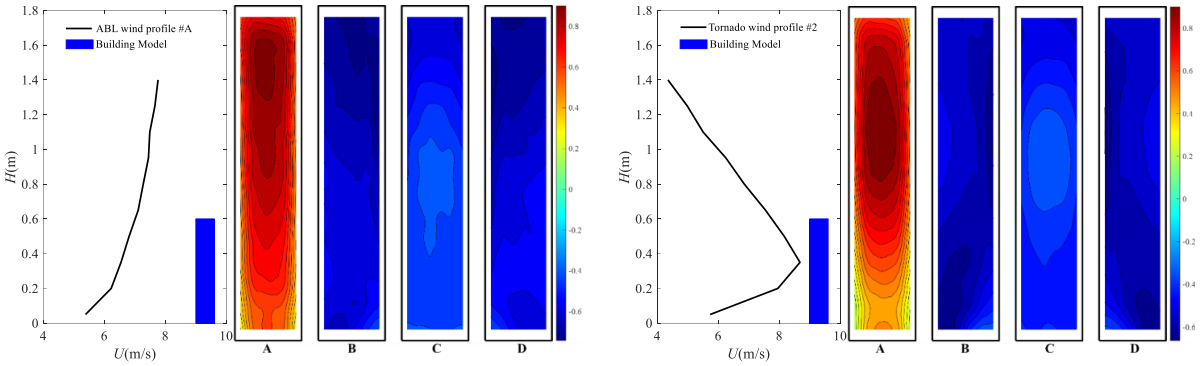

Figure 2. Mean wind pressure coefficient distribution

3.2. Interlayer wind force coefficient

FIG.3 shows the variation of mean interlayer wind force coefficients in height for different wind directions under two wind profiles. It shows that the difference in the interlayer along-wind (X-direction) force coefficients between the two wind profiles is not significant, regardless of wind direction. However, the most unfavourable position corresponding to largest along-wind force coefficients for the non-synoptic wind profile is slightly lower than that for the synoptic wind profiles.

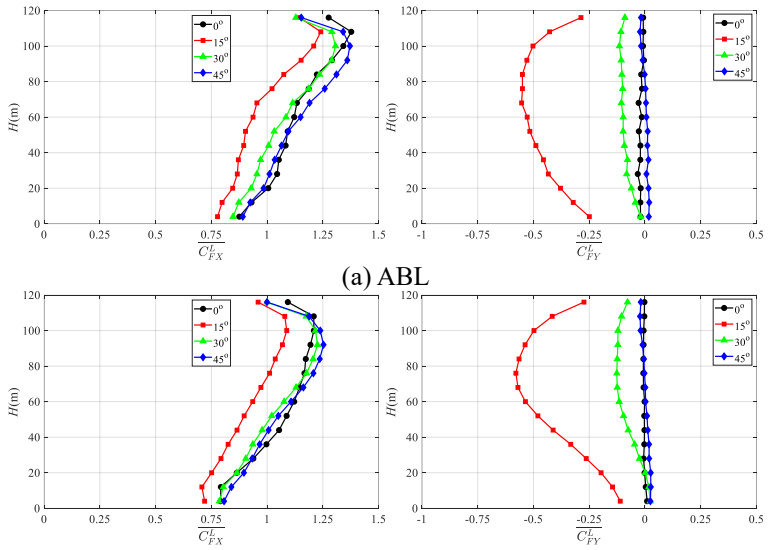

Figure 3. Mean interlayer wind force coefficient distribution for different wind direction.

In addition, the along-wind force coefficients at wind direction of 15° is significantly smaller than those for other wind directions. Meanwhile, the magnitudes of interlayer cross-wind (Y-direction) force coefficients at this wind direction are greater than those for other wind directions. The most unfavourable value of cross-wind force coefficients (in magnitude) at 15° for non-synoptic wind profile is slightly larger than those for the synoptic wind profile, while the values at the bottom of the building for the non-synoptic wind profile are slightly smaller, which results in significant

variations of cross-wind force coefficients in the vertical direction for the non-synoptic wind profile. The difference in the most unfavourable values is mainly due to the large difference in wind speed between the two wind profiles at their corresponding locations.

3.3. Overall wind force coefficient

FIG.4 shows the variation of mean and peak overall wind force coefficients due to wind direction for different wind profiles. Both the mean and peak results for the non-synoptic wind profiles are smaller than the results for the synoptic wind profiles, and the difference remained within 10%; Meantime, the results of two wind profiles reach the maximum value at 0° and the minimum value at 20° together. However, the results do not fluctuate drastically, and the amplitude stays within 20%.

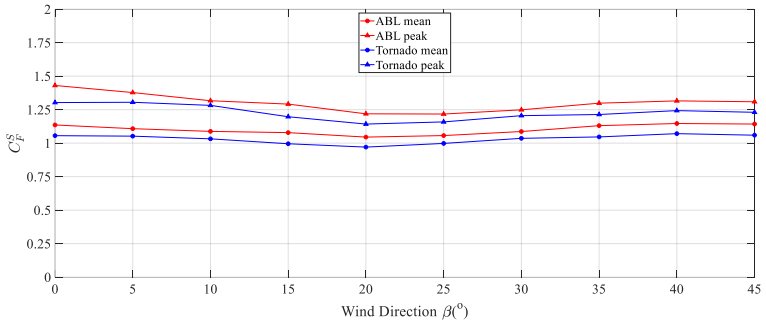

Figure 4. Variation of mean and peak overall wind force coefficients due to wind direction.

4. CONCLUSION

1) There is a significant difference in the distribution of wind pressure coefficients on the building surface under the synoptic and non-synoptic wind profiles.
2) The cross-wind interlayer wind force coefficient is significantly larger at 15° than at the other wind direction, while the most unfavourable values for the non-synoptic wind profiles are larger than those for the synoptic ones.
3) The overall wind force coefficients under two wind profiles reach their maximum and minimum value at same wind direction.

ACKNOWLEDGEMENTS

This study is funded by the Natural Science Foundation of China (NSFC) (Grant No. 51878504 and 52178502), and the Research Foundation of State Key Laboratory of Disaster Reduction in Civil Engineering (Grant No. SLDRCE19-B-01), which is gratefully acknowledged.

REFERENCES

El Damatty, A. A., & Hamada, A. (2016). F2 tornado velocity profiles critical for transmission line structures. *Engineering Structures*, *106*, 436–449.

Hamada, A., El Damatty, A. A., Hangan, H., & Shehata, A. Y. (2010). Finite element modelling of transmission line structures under tornado wind loading. *Wind and Structures*, *13*(5), 451–469.

Kashefizadeh, M. H., Verma, S., & Selvam, R. P. (2019). Computer modelling of close-to-ground tornado wind-fields for different tornado widths. *Journal of Wind Engineering and Industrial Aerodynamics*, *191*, 32–40.

Zhang, Y., Sarkar, P., & Hu, H. (2014). An experimental study on wind loads acting on a high-rise building model induced by microburst-like winds. *Journal of Fluids and Structures*, *50*, 547–564.